Determination of Turbofan Inlet Acoustics Using Finite Elements

R. K. Sigman*, R. K. Majjigi†, and B.T. Zinn‡
Georgia Institute of Technology, Atlanta, Ga.

This paper describes the application of the finite-element method in combination with Galerkin's method in the determination of the acoustic properties of turbofan inlets containing high subsonic Mach number steady flows. An approximate solution for the steady inviscid flowfield is obtained using an integral method for calculating the potential flowfield in the inlet with a correction to account for compressibility effects. The accuracy of the finite element technique in predicting the acoustic properties of annular ducts has been checked by comparison with available analytical solutions for the problems of plane and spinning wave propagation through a hard-walled annular duct with a constant mean flow. Results are presented comparing low-frequency plane wave propagation through a hard-walled turbofan inlet containing a one-dimensional steady flow with the same inlet containing a fully two-dimensional axisymmetric steady flow. It is shown that when one-dimensional steady flow is assumed to exist in the duct, the plane wave propagates with relatively little distortion. However, propagation of a plane wave through the fully two-dimensional flowfield in the inlet produces severe distortion due to the excitation of higher order modes.

Introduction

THE imposition of strict federal regulations upon the noise environment produced by various aeronautical and industrial systems calls for the development of efficient analytical solution techniques that would enable the designer to better understand the acoustic properties of the system under consideration. Many of these systems contain odd-shaped duct configurations carrying multidimensional mean flows, with or without acoustic treatments along their walls. Examples of such applications include various components of air-breathing engines, wind tunnels, turbomachinery, air-conditioning equipment, and so on. It is believed that the development of a reliable analytical technique for predicting the acoustic properties of the above mentioned duct configurations will undoubtedly improve existing noise reduction design procedures that generally involve costly cut-and-try test and development programs. The development of such an analytical solution technique, utilizing the finite-element method (FEM) is the subject of this paper. An extensive survey of the acoustics of aircraft inlets has been presented by Nayfeh et al,[1] including a comprehensive bibliography. Of particular interest are the use of numerical methods such as finite differences[2] and integral techniques[3] in the study of acoustic propagation in variable area hard-walled ducts without mean flow. Due to the additional complications created by the presence of a steady flow, most studies of sound propagation in annular ducts with varying cross-sectional area containing a mean flow employ one or more simplifying assumptions, such as one-dimensional mean flow,[4] quasi-one-dimensional mean flow,[5] or slowly varying cross-sectional area.[6] In many instances, however, practical considerations call for the use of relatively short ducts having large transverse and streamwise velocity gradients. Under such conditions, the predictions of existing theoretical approaches, in which the mean flow is assumed to be one-dimensional or nearly one-dimensional, is open to question. Thus, there is a need for an analytical method that can determine the acoustics of duct systems involving multidimensional flows.

Since the original presentation of this research[7] in January 1977, several other applicaitons of finite element methods to duct acoustics[8-10] have been reported. Of particular interest is the work of Abrahamson,[10] who also used finite elements to predict sound propagation in an axisymmetric duct containing a compressible steady flow.

The research described in this paper was initiated for the purpose of predicting the acoustics properties of turbofan inlets carrying high subsonic Mach number mean flows. To achieve this objective, it is necessary to develop solution techniques that are capable of predicting the acoustic properties of variable area, annular ducts with or without acoustic treatments along their walls, subjected to a variety of practical sound excitation conditions. Such a solution technique should be capable of properly accounting for the reflection processes at the inlet entrance plane, the space dependence of the noise source at the fan plane (see Fig. 1), the odd shape geometry of the duct under consideration, the multidimensionality of the steady flow, and the mixed boundary conditions (e.g., partial lining) at the duct walls. The preceding requirements obviously preclude the development of an analytical solution for the duct under consideration and one must resort to the development of an efficient numerical solution approach. It will be shown in this paper that the application of the finite element method (FEM) (see Ref. 11 for a general discussion of this method), in conjunction with the method of weighted residuals, can indeed provide the needed solutions.

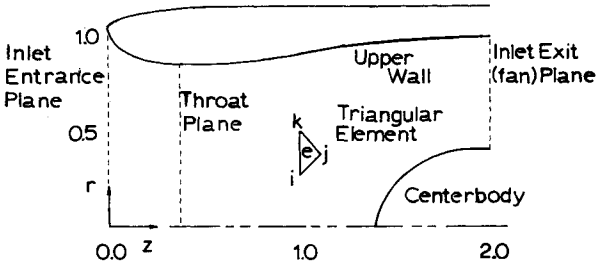

Fig. 1 Turbofan inlet geometry.

Presented as Paper 77-18 at the AIAA 15th Aerospace Sciences Meeting, Los Angeles, Calif., Jan. 24-26, 1977; submitted Sept. 26, 1977; revision received July 11, 1978. Copyright © American Institute of Aeronautics and Astronautics, Inc., 1977. All rights reserved.

Index category: Aeroacoustics.

*Research Engineer. Member AIAA.

†Graduate Research Asssistant, School of Engineering.

‡Regents' Professor, School of Engineering. Associate Fellow AIAA.

Formulation of the Problem

To develop the needed solution technique, the problems of acoustic wave propagation through the duct configuration shown in Fig. 1 will be considered. The flow in the duct is assumed to be inviscid, non-heat-conducting, and irrotational. Although these assumptions exclude consideration of the effects of boundary layers in the mean flow on the acoustic properties, it assures the existence of a velocity potential with a corresponding decrease in the number of dependent variables. Body forces are neglected. To derive the needed nondimensional conservation equations, velocities, lengths, and time are respectively normalized with respect to the sound speed at stagnation conditions c_o^*, the duct radius d_r^*, and d_r^*/c_o^*. The density ρ and pressure p are respectively normalized with the stagnation density ρ_o^* and $\rho_o^* c_o^{*2}$. The velocity potential φ is normalized with respect to $c_o^* d_r^*$ and the frequency with respect to c_o^*/d_r^*. Under these conditions, it can be shown[12] that the behavior of the flow in the duct is described by the following nonlinear partial differential equation for the flow potential φ:

$$\frac{\partial^2\varphi}{\mathrm{d}t^2} + \frac{\partial}{\partial t}(\nabla\varphi\cdot\nabla\varphi) + \tfrac{1}{2}\nabla\varphi\cdot\nabla(\nabla\varphi\cdot\nabla\varphi) = c^2\nabla^2\varphi \quad (1)$$

where

$$c^2 = 1-(\gamma-1)\left[\frac{\partial\varphi}{\partial t} + \tfrac{1}{2}\nabla\varphi\cdot\nabla\varphi\right]$$

and γ is the ratio of specific heats. Rewriting Eq. (1) in a cylindrical coordinate system (i.e., r, θ, z) with the z axis coinciding with the turbofan inlet axis yields:

$$\begin{aligned} c^2\left\{\varphi_{rr}+\frac{\varphi_r}{r}+\frac{\varphi_{\theta\theta}}{r^2}+\varphi_{zz}\right\} - \varphi_{tt} &= 2\varphi_r\varphi_{tt} + \frac{2\varphi_\theta\varphi_{\theta t}}{r^2} \\ &+ 2\varphi_z\varphi_{zt} + {\varphi_r}^2\varphi_{rr} + \frac{{\varphi_\theta}^2\varphi_{\theta\theta}}{r^4} + {\varphi_z}^2\varphi_{zz} + \frac{2\varphi_r\varphi_\theta\varphi_{r\theta}}{r^2} \\ &+ 2\varphi_r\varphi_z\varphi_{rz} + \frac{2\varphi_z\varphi_\theta\varphi_{z\theta}}{r^2} - \frac{\varphi_r{\varphi_\theta}^2}{r^3} \end{aligned} \quad (2)$$

where the subscripts indicate partial differentiation with respect to the subscripted variables.

To obtain the needed acoustic solutions, the flow potential is rewritten as the sum of a steady axisymmetric mean flow potential $\bar{\varphi}(r,z)$ and an acoustic potential $\varphi'(r,\theta,z,t)$; that is

$$\varphi(r,\theta,z,t) = \bar{\varphi}(r,z) + \varphi'(r,\theta,z,t) \quad (3)$$

Because of the rotational nature of the fan and compressor,[13] they tend to generate sound that is characterized by spinning acoustic modes. In order to account for spinning modes, the acoustic potential is assumed to have the following form:

$$\varphi'(r,\theta,z,t) = \Phi(r,z)e^{-i(\omega t - m\theta)} \quad (4)$$

where $\Phi(r,z)$ is a complex quantity; that is,

$$\Phi = \bar{\varphi} + i\hat{\varphi} \quad (5)$$

Substitution of Eq. (3) into Eq. (2) produces a lengthy equation consisting of three types of terms: 1) terms containing only products of steady or mean flow quantities, 2) products of mean flow quantities and acoustic quantities, and 3) products of acoustic quantities. Using the standard assumptions of perturbation analyses, the mean flow is assumed to be undisturbed by the presence of the acoustic perturbations. Thus, the terms containing only products of mean flow quantities represent the governing equation for the mean flow which is equal to zero. Furthermore, products of acoustic quantities are neglected in comparison to products of mean and acoustic quantities. The remaining equation, consisting of the products of the mean and acoustic quantities is referred to as the linearized acoustic equation. Substituting Eqs. (4) and (5) into the linearized acoustic equation and separating the resulting equation into its real and imaginary parts leads to derivation of the following two linear coupled, partial differential equations for $\bar{\varphi}$ and $\hat{\varphi}$:

$$\begin{aligned} &[\bar{c}^2-\bar{\varphi}_r^2]\bar{\varphi}_{rr} + [\bar{c}^2-\bar{\varphi}_z^2]\bar{\varphi}_{zz} - 2\bar{\varphi}_r\bar{\varphi}_z\bar{\varphi}_{rz} \\ &+ [-(\gamma+1)\bar{\varphi}_{rr}\bar{\varphi}_r - 2\bar{\varphi}_{rz}\bar{\varphi}_z + (\bar{c}^2/r) \\ &- (\gamma-1)(\bar{\varphi}_r^2/r) - (\gamma-1)\bar{\varphi}_r\bar{\varphi}_{zz}]\bar{\varphi}_r + [-(\gamma+1)\bar{\varphi}_{zz}\bar{\varphi}_z \\ &- 2\bar{\varphi}_{rz}\bar{\varphi}_r - (\gamma-1)\bar{\varphi}_{rr}\bar{\varphi}_z - (\gamma-1)(\bar{\varphi}_z\bar{\varphi}_r/r)]\bar{\varphi}_z \\ &+ [\omega^2 - m^2(\bar{c}^2/r^2)]\bar{\varphi} - 2\omega\bar{\varphi}_r\hat{\varphi}_r - 2\omega\bar{\varphi}_z\hat{\varphi}_z \\ &- \omega(\gamma-1)[\bar{\varphi}_{rr} + (\bar{\varphi}_r/r) + \bar{\varphi}_{zz}]\hat{\varphi} = 0 \end{aligned} \quad (6)$$

$$\begin{aligned} &[\bar{c}^2-\bar{\varphi}_r^2]\hat{\varphi}_{rr} + [\bar{c}^2-\bar{\varphi}_z^2]\hat{\varphi}_{zz} - 2\bar{\varphi}_z\bar{\varphi}_r\hat{\varphi}_{rz} \\ &+ [-(\gamma+1)\bar{\varphi}_{rr}\bar{\varphi}_r - 2\bar{\varphi}_{rz}\bar{\varphi}_z + (\bar{c}^2/r) - (\gamma-1)(\bar{\varphi}_r^2/r) \\ &- (\gamma-1)\bar{\varphi}_r\bar{\varphi}_{zz}]\hat{\varphi}_r + [-(\gamma+1)\bar{\varphi}_{zz}\bar{\varphi}_z - 2\bar{\varphi}_{rz}\bar{\varphi}_r \\ &- (\gamma-1)\bar{\varphi}_{rr}\bar{\varphi}_z - (\gamma-1)(\bar{\varphi}_z\bar{\varphi}_r/r)]\hat{\varphi}_z \\ &+ [\omega^2 - m^2(\bar{c}^2/r^2)]\hat{\varphi} + 2\omega\bar{\varphi}_r\bar{\varphi}_r + 2\omega\bar{\varphi}_z\bar{\varphi}_z \\ &+ \omega(\gamma-1)[\bar{\varphi}_{rr} + (\bar{\varphi}_r/r) + \bar{\varphi}_{zz}]\bar{\varphi} = 0 \end{aligned} \quad (7)$$

where

$$\bar{c}^2 = 1-[(\gamma-1)/2][\bar{\varphi}_r^2 + \bar{\varphi}_z^2]$$

It should be pointed out that in the development of Eqs. (6) and (7) the following expression for the sound velocity perturbation $(c^2)'$ has been used:

$$(c^2)' = -(\gamma-1)[-i\omega\varphi' + \bar{\varphi}_z\varphi_z' + \bar{\varphi}_r\varphi_r']$$

Since the steady flow is axisymmetric, the equation expressing the conservation of acoustic momentum in the θ direction can be integrated to give a relationship between the pressure and velocity potential:

$$p' = -\bar{\rho}(-i\omega\varphi' + \bar{\varphi}_z\varphi_z' + \bar{\varphi}_r\varphi_r') \quad (8)$$

Before proceeding with the solution of the equations, the geometry and boundary conditions for the problem under consideration must be established. The geometry of a typical turbofan inlet is shown in Fig. 1 where, due to geometry of the inlet, only a single meridional plane is shown. The boundary of the inlet may be divided into three distinct sections, each described by a different boundary condition. The inlet exit plane represents the interface between the inlet and the remainder of the engine; it is referred to as the inlet exit plane as it is the location where the steady flow leaves the inlet. This plane also represents the location at which the fan/compressor noise is introduced into the inlet. In view of the previously mentioned spinning nature of the sound excitation at the inlet exit plane, the boundary condition describing the normal acoustic velocity φ_z' at this plane can be expressed in the following form:

$$\varphi_{z_{\text{exit}}}' = f(r)e^{-i(\omega t - m\theta)} \qquad f(r) = f_r(r) + if_i(r) \quad (9)$$

where the complex quantity $f(r)$ describes the r dependence of the source. Using Eqs. (4) and (5), Eq. (9) can be written as

follows:

$$\tilde{\varphi}_{z_{\text{exit}}} = f_r(r) \tag{10}$$

$$\hat{\varphi}_{z_{\text{exit}}} = f_i(r) \tag{11}$$

For the study of axisymmetric plane wave propagation, (i.e., $m=0$) the condition $f(r)$ = a constant applies. For a more general excitation, an appropriate combination of higher order spinning modes, (i.e., Bessel functions) must be used to describe the sound source.

Since in the present paper the duct boundaries are taken to be hard walls, the appropriate boundary condition at these locations is:

$$\varphi_n' = 0$$

The preceding boundary condition reduces into the following two real relationships expressed in terms of the radial and axial velocity components:

$$\tilde{\varphi}_r \cos\alpha - \tilde{\varphi}_z \sin\alpha = 0 \tag{12}$$

$$\hat{\varphi}_r \cos\alpha - \hat{\varphi}_z \sin\alpha = 0 \tag{13}$$

where α is the angle of inclination of the duct wall with respect to the z axis.

Due to the complex nature of the reflection process at the inlet entrance plane, the precise form of the boundary condition at this location is currently not known. Rice[14] has argued that except for modes near cutoff frequencies, the assumption of no reflection of "internal" duct waves at the inlet entrance plane is a reasonable one. As the primary objective of the present analysis is the development of the needed solution technique, the inlet entrance plane boundary condition in the present study is specified in the following form:

$$p' = -\bar{\rho}\bar{c}Z\varphi_z' \tag{14}$$

where $\bar{\rho}$ and $\bar{c}$ are the local steady flow density and sound speed at the entrance plane and Z is the local impedence. The analytical solution for the propagation of a single acoustic mode, with cutoff frequency, β, in a cylindrical or annular duct with constant mean flow velocity, $\bar{\varphi}_z$, is known. This solution provides the following impedance condition for transmission of a single acoustic mode without reflection:

$$Z = \frac{\omega\bar{c} + \bar{\varphi}_z\sqrt{\omega^2 - \beta^2(\bar{c}^2 - \bar{\varphi}_z^2)}}{\omega\bar{\varphi}_z + \bar{c}\sqrt{\omega^2 - \beta^2(\bar{c}^2 - \bar{\varphi}_z^2)}}$$

and values of β are available in Ref. 13. For plane waves, the cutoff frequency β equals zero and the more familiar result $Z=1$ is obtained. Since in the inlet case the steady flow velocity is not uniform at the inlet entrance plane, there will be a partial reflection of the principle mode. Furthermore, any additional modes excited by duct cross-sectional area variations and steady flow velocity gradients will also be partially reflected. Improved inlet plane boundary conditions will be input into the developed computer programs as they become available. Application of Eq. (8) to Eq. (14) yields the following equivalent boundary conditions:

$$\omega\hat{\varphi} + \bar{\varphi}_r\tilde{\varphi}_r + (\bar{\varphi}_z - \bar{c}Z)\tilde{\varphi}_z = 0 \tag{15}$$

$$-\omega\tilde{\varphi} + \bar{\varphi}_r\hat{\varphi}_r + (\bar{\varphi}_z - \bar{c}Z)\hat{\varphi}_z = 0 \tag{16}$$

Methods of Solution

Inlet Steady Flow

Analytical solutions for the nonlinear equations describing the steady compressible flow in axisymmetric, axially nonuniform passages are not generally available and complex numerical solution approaches must be employed to obtain the desired flow description. Since the main objective of the current study is the description of the acoustic flowfield, for which the steady flow is needed as input, an approximate solution was used to obtain the needed steady inlet flow description. The approximate steady flow computation consists of a potential flow solution with a correction accounting for compressibility effects. An integral solution technique was used to compute the inlet potential flow utilizing a computer program developed earlier at Georgia Tech,[15] and Lieblein's correction[16] was utilized to account for compressibility effects.

The potential flow is governed by Laplace's equation and is subject to boundary conditions specifying the magnitude of the velocity normal to the inlet. The component of velocity normal to the solid surfaces of the inlet must be zero. The suction effect of a fan or compressor can be simulated by prescribing a finite velocity distribution over the inlet exit plane. Using the method developed by Hess and Smith,[17] the inlet surface is subdivided into a large number of straight-line segments. Each segment consists of a distributed source or sink of uniform, but as yet undetermined, strength. By requiring that the boundary condition be satisfied at the midpoint of each element, the individual source strengths are determined.

Using the principle of superposition, the velocity component normal to the inlet surface due to the surface source and a freestream velocity are expressed in the following integral form of Laplace's equation:

$$2\pi\sigma(q) - \int_{S_A} \frac{\partial}{\partial n}\left[\frac{1}{R(q,t)}\right]\sigma(t)\,dS_A + \vec{V}_\infty \cdot \vec{n}\,|_q = V_n \tag{17}$$

where σ is the unknown source strength on each surface element. The first term in Eq. (17) is the velocity normal to the body surface induced at q (the midpoint of an element) by the source at q. The second term is the velocity component normal to the body surface at point q due to the sources and sinks distributed over the remainder of the body surface. The quantity $\partial/\partial n\ [(1/R(q,t))]$, where $R(q,t)$ is the distance between points q and t, depends only on the geometry of the surfaces. $V_\infty \cdot n$ is the component of the freestream velocity normal to the surface at q. The term on the right side, V_n, is the specified component of the fluid velocity normal to the inlet surface at q and is a known function of position. The normal velocity component V_n is zero for solid boundaries and is equal to $V_F(r)$ at the fan plane.

The foregoing integral equation is reduced to a set of linear algebraic equations which are then solved by matrix methods. The velocities on and off the inlet surfaces are calculated from the computed source distribution.

Next, since the inlet will be operating at high subsonic Mach numbers, the incompressible solution within the inlet is corrected to account for compressibility effects using the semiempirical equation proposed by Lieblein and Stockman[16]; that is,

$$V_c = V_i\left(\frac{\rho_i}{\bar{\rho}}\right)^{\frac{V_i}{\bar{V}_i}} \tag{18}$$

where V_c is the "compressible" velocity, V_i is the previously computed incompressible velocity, $\bar{V}_i$ is the average incompressible velocity across the inlet flow passage, ρ_i is the incompressible density (equal to the compressible stagnation density), and $\bar{\rho}$ is the average compressible density across the inlet flow passage. The corrected mean flow solution is then used as an input in the inlet acoustic analysis.

Finite Element Solution of the Acoustic Equations

Due to its apparent advantages, the application of the FEM in the solution of a variety of engineering problems has been

rapidly growing in recent years. A detailed discussion of the FEM can be found in Ref. 11. Due to its suitability for handling problems involving complex geometries and mixed boundary conditions, the FEM is used in the present investigation in the solution of the inlet wave equations.

To obtain the needed solutions, Eqs. (6) and (7), which describe the wave propagation in the inlet, have been transformed into integral equations, utilizing the Galerkin method. The resulting integral equations were then solved using the FEM. The solution involves the following six operations:

Subdivision of the Solution Domain

The domain of interest (in this case, the inlet duct) is subdivided into a prescribed number of triangular elements. The vertices of each triangle are nodal points or nodes, and the assembly of nodes and triangles are given an ordered set of numbers. The node and element number sets are then catalogued so that each element number corresponds to three nodal numbers and each nodal number is associated with a fixed number of elements whose number may vary between one and six depending upon the node location. A computer code has been developed which subdivides a duct into triangles and catalogues the geometric nodal locations, nodal numbers, and element numbers.

Selection of Interpolation Functions

The acoustic velocity potential is assumed to vary linearly over the eth element, as described by the following relationships (see Fig. 1):

$$\tilde{\varphi}(r,z) = N_i^e(r,z)\tilde{\varphi}_i + N_j^e(r,z)\tilde{\varphi}_j + N_k^e(r,z)\tilde{\varphi}_k \tag{19}$$

$$\hat{\varphi}(r,z) = N_i^e(r,z)\hat{\varphi}_i + N_j^e(r,z)\hat{\varphi}_j + N_k^e(r,z)\hat{\varphi}_k \tag{20}$$

where $\tilde{\varphi}_i$ is the to be determined value of φ at the ith nodal point, etc., and

$$N_i^e = [a_i + b_i z + c_i r]/2\Delta$$

where

$$\begin{aligned} a_i &= z_j r_k - z_k r_j \\ b_i &= r_j - r_k \\ c_i &= z_k - z_j \end{aligned} \tag{21}$$

and

$$\Delta = \text{area of the } e\text{th element}$$

Similar expressions can also be obtained for N_j and N_k by cyclic rotation of the subscripts i, j, and k. For a complete description of the properties of the element interpolating functions see Ref. 11.

Establishing Elemental Relations

The Galerkin method is applied to the governing differential equations and boundary conditions to develop the matrix equations that express the properties of individual elements in terms of the unknown nodal values. Denoting either of the partial differential equations, Eq. (6) or (7), by the operator $L(\varphi')$, application of the Galerkin and FEM methods[11] yields the following relationships:

$$\sum_{e=1}^{E} \int\int_{\Delta^{(e)}} \int N_m^e L(\varphi')\, dv^{(e)} = 0 \qquad m = 1,2,\ldots N \tag{22}$$

where the integration is performed over each element. In Eq. (22), N is the total number of nodes in the problem under consideration and E is the number of elements. It should be noted that N_m^e is zero for all elements not having the nodal point, m, as a vertex. Equation (22) provides $2N$ equations for the $2N$ unknown nodal values.

There exists[11] a mathematical restriction in the choice of interpolating functions stating that the values of φ' and its partial derivatives up to the highest order appearing in Eq. (22) must have representation as the element size shrinks to zero. Since linear interpolating functions have been chosen in the present study, the second-order partial derivatives of φ' will be zero. Rather than choose higher order interpolating functions, all terms in Eq. (22) containing second-order partial derivatives of φ' are reduced to terms containing first-order derivatives of φ' using Green's theorem in the plane.[18] The boundary conditions, given in the previous section, are introduced into the FEM equations through boundary integrals that are obtained as a result of the previously mentioned use of Green's theorem. For the problem at hand, four different elemental relations have been developed, depending upon the location of the triangles under consideration; that is, 1) triangles interior to the flow region, 2) triangles adjacent to a hard wall, 3) triangles adjacent to the entrance plane, and 4) triangles adjacent to the exit plane.

Assembly of Element Equations to Obtain a System of Algebraic Equations

Based on the ordering system defined in the first step, the individual element equations are combined into a matrix equation describing the properties of the potential φ' in the domain under study. Since each node is only affected by adjacent elements, the resulting matrix is banded.

Solution of the System Equations

A considerable amount of information is currently available about the solution of large, banded matrices. In the present study, two CDC subroutines and one IMSL subroutine for the solution of banded matrices have been compared for speed and accuracy. All three subroutines provide comparable accuracy, and CDC subroutine BLSWNP is used for routine calculations.[19] These computer subroutines employ a condensed storage scheme which results in considerable savings in computer memory and computation times.

Additional Calculations

Once the velocity potential is obtained at the nodes, additional variables such as the axial and radial velocities and acoustic pressure can be calculated at any point in the domain, by utilizing the computed solutions for φ together with Eqs. (19) and (20).

Results

Steady Flow Calculations

To predict the acoustic properties of a practical inlet configuration, an inlet geometry investigated in Ref. 20 has also been chosen for the present study. However, before proceeding with the inlet acoustic analysis, the behavior of the inlet steady flow must be determined.

Since obtaining an exact description of the inlet mean flow was beyond the scope of the present study, an approximate approach has been undertaken to obtain the desired mean flow solution. In this approach, an earlier developed computer program was utilized to obtain a solution for the incompressible flow in the inlet, and Eq. (18) was utilized to apply the needed compressibility correction. As explained earlier in this paper, the incompressible solution was obtained by solving an integral formulation of Laplace's equation with the inlet boundary divided into 142 straight-line segments. The resulting solution provided descriptions of the source strengths and velocities at the inlet boundaries and the velocities at the inlet interior. The chosen freestream and fan

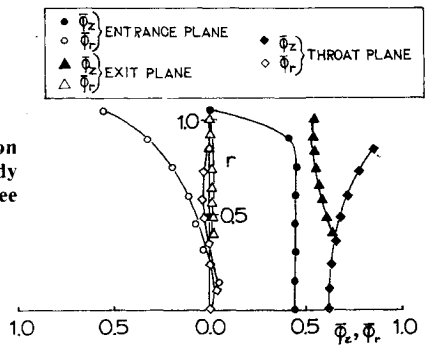

Fig. 2 Radial variation of compressible steady flow velocities at three axial locations.

plane velocities correspond to a freestream Mach number of 0.12 and an inlet mass flow rate of 11.96 kg/s.[20]

"Compressible" velocity profiles at the inlet entrance plane, the throat and the fan plane are shown in Fig. 2 for the specified conditions. Such computations were performed at other axial locations and these calculations provide the mean flow input needed for the solution of the acoustic equations.

Acoustic Calculations

To check the accuracy of the developed FEM computer program, solutions for the problems of plane and spinning wave propagation through a hard-walled annular duct with constant mean flow have been obtained for comparison with available analytical solutions. For this case, the same equations, Eqs. (6) and (7), reduce to the following form:

$$\tilde{\varphi}_{rr}+\frac{\tilde{\varphi}_r}{r}+(1-M^2)\tilde{\varphi}_{zz}+\left(\omega^2-\frac{m^2}{r^2}\right)\tilde{\varphi}-2\omega\hat{\varphi}_z=0 \qquad (23)$$

$$\hat{\varphi}_{rr}+\frac{\hat{\varphi}_r}{r}+(1-M^2)\hat{\varphi}_{zz}+\left(\omega^2-\frac{m^2}{r^2}\right)\hat{\varphi}+2M\omega\tilde{\varphi}_z=0 \qquad (24)$$

where ω is the angular frequency (now nondimensionalized by the outer annulus radius and the ambient sound speed), m is the spinning mode number, and M is the constant mean flow Mach number.

The hard-wall boundary conditions are described by the following expressions:

$$\left.\begin{aligned}\tilde{\varphi}_r&=0\\ \hat{\varphi}_r&=0\end{aligned}\right\}\text{ at }\begin{cases} r=\sigma\,(\text{inner wall})\\ r=1\,(\text{outer wall})\end{cases} \qquad (25)$$

and the sound source boundary condition at the exit plane (i.e., $z=L$) is given by:

$$\tilde{\varphi}_z=-f(r) \qquad \hat{\varphi}_z=0 \qquad (26)$$

Assuming no reflection at the duct entrance plane where $z=0$, the following boundary condition applies:

$$\tilde{p}=-Z\tilde{\varphi}_z \qquad \hat{p}=-Z\hat{\varphi}_z \qquad (27)$$

The needed expressions for the impedance Z and $f(r)$ are given below. The exact solution to this problem is given by:

$$\tilde{\varphi}=-(f(r)/k)\sin[k(z-L)] \qquad (28)$$

and

$$\hat{\varphi}=-(f(r)/k)\cos[k(z-L)] \qquad (29)$$

For the axisymmetric plane wave case (i.e., $m=0$) the various quantities in Eqs. (26-29) take on the following form:

$$f(r)=1 \qquad Z=1 \qquad k=\omega/(1-M) \qquad (30)$$

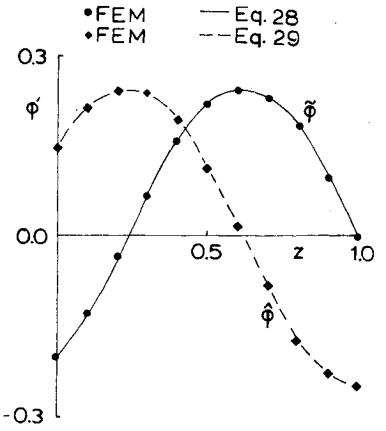

Fig. 3 Comparison of acoustic velocity potential for plane wave propagation in an annular cylinder ($M=0.5$, $\omega=2.0$).

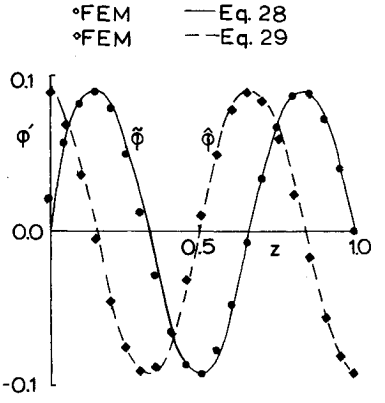

Fig. 4 Comparison of the acoustic velocity potential for spinning wave propagation in an annular cylinder ($M=0.5$, $\omega=6.0$).

The real and imaginary components of the velocity potential, as calculated by the FEM for an annular cylinder with $\sigma=0.5$ and $L=1$, are compared with the exact values computed using Eqs. (28) and (29) in Fig. 3 for the case of $M=0.5$ and $\omega=2.0$. A good agreement between the FEM and analytical solutions is shown; good agreement has also been obtained when the predictions for the acoustic velocities and pressures were compared.

The expressions describing the propagation of a spinning wave with lobe number m and radial mode μ are:

$$f(r)=E_{m_\mu}{}^{(\sigma)}(\beta r) \qquad Z=\frac{\omega+M\sqrt{\omega^2-\beta^2(1-M^2)}}{\omega M+\sqrt{\omega^2-\beta^2(1-M^2)}} \qquad (31)$$

and

$$k=\frac{M\omega+\sqrt{\omega^2-\beta^2(1-M^2)}}{1-M^2}$$

where $E_{m_\mu}{}^{(\sigma)}$ and β ($=k_{m_\mu}{}^{(\sigma)}$ in Ref. 13) are tabulated in Ref. 13.

Results of FEM calculations for the velocity potential in the previously described annular duct with $m=4$, $\mu=0$, $\omega=6.0$, and $M=0.5$ are presented in Fig. 4. The analytical solutions, given by Eqs. (28) and (29) are also shown in Fig. 4 and good agreement between the two solutions is noted. Similar comparisons for other acoustic variables, such as acoustic velocity and pressure, have also shown good agreement.

For the FEM calculations, the duct was subdivided into 220 triangles with 136 nodes. For a Mach number of 0.5, very good agreement between FEM calculations and the exact solution was obtained for values of ω up to 10. At this point ($\omega=10$, $M=0.5$), there are about six nodes per wave length at any radial location. Clearly, the accuracy lost at higher frequencies can be recovered by a finer element subdivision or, possibly, a more elaborate description of the dependent variable φ.

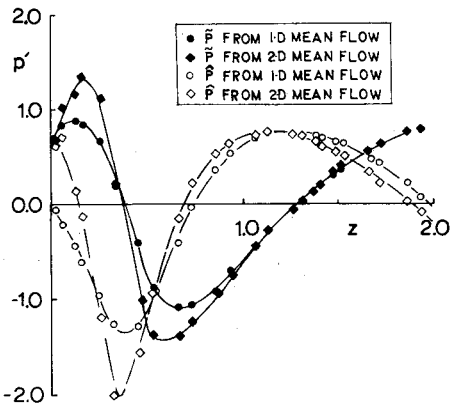

Fig. 5 Acoustic pressure distribution along the inlet upper wall ($\omega = 1.0$, axisymmetric plane wave excitation).

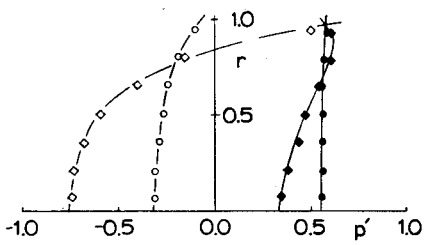

Fig. 6 Radial variation of acoustic pressure at the entrance plane for $\omega = 1.0$ (symbols defined in Fig. 5).

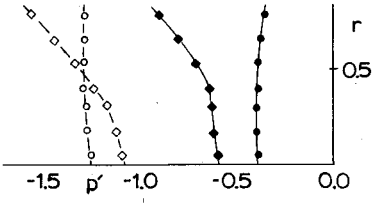

Fig. 7 Radial variation of acoustic pressure at the throat plane for $\omega = 1.0$ (symbols defined in Fig. 5).

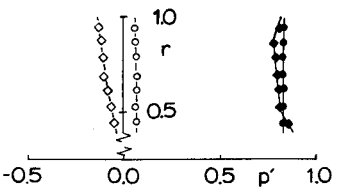

Fig. 8 Radial variation of acoustic pressure at the inlet exit (fan) plane for $\omega = 1.0$ (symbols defined in Fig. 5).

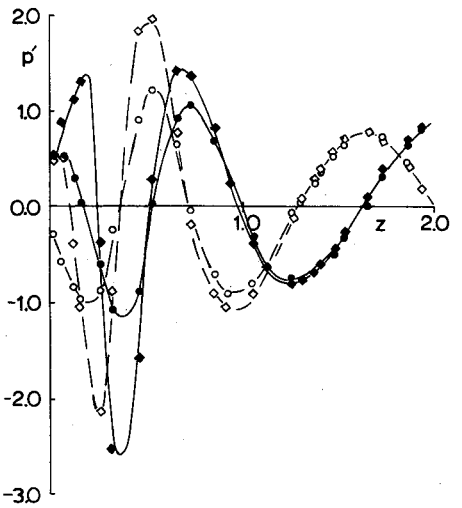

Fig. 9 Acoustic pressure distribution along the inlet upper wall ($\omega = 2.0$, axisymmetric plane wave excitation, symbols defined in Fig. 5).

Improved accuracy at high frequencies can also be obtained by using the generalized wave envelope transformation.[21] A new variable, Ψ, defined as

$$\Psi(r,z) = e^{i\delta z}\varphi'(r,z) \tag{32}$$

where δ is a free constant, is substituted into Eqs. (23-26) to form a new set of governing partial-differential equations and boundary conditions for the variable Ψ. If the constant δ is taken to equal the appropriate wave number k [see Eq. (30) or (31)], the analytical solution for Ψ is:

$$\Psi(r) = [if(r)/k]e^{ikL} \tag{33}$$

which does not vary in the axial direction. FEM calculations have been carried out using the wave envelope equation and the results compare with the predictions of Eq. (33) to four decimal places. It should be noted that the wave envelope transformation is useful when wave propagation in a single axial direction is important, since reflected waves are not well preserved.

The acoustic calculations for the turbofan inlet shown in Fig. 1 were performed at two frequencies using two different descriptions for the inlet steady flowfield. The calculation of the more accurate two-dimensional steady flowfield has already been described in a previous section. In order to investigate the effects of the two-dimensional nature of the mean flow on the acoustic propagation in the inlet, the mean flow was also computed using a one-dimensional, isentropic compressible flow model[22] to describe the inlet mean flow. As in the two-dimensional flow computations, a freestream Mach number of 0.12 and an inlet mass flow rate of 11.96 kg/s have also been used in the one-dimensional flow computations. The solution domain, consisting of the inlet duct, has been subdivided into 360 triangles with 212 nodes. The real and imaginary parts of the acoustic potential were calculated at the nodes, and the real and imaginary parts of the acoustic axial and radial velocity components and the acoustic pressure were calculated at the centroids of the triangular elements using the linear interpolation functions for the acoustic potential [i.e., see Eq. (21)].

Calculations for axisymmetric plane wave excitation (i.e., $m = 0$) at the inlet exit plane and the frequency $\omega = 1$ and 2 have been performed using the one- and two-dimensional steady flow calculations. Figure 5 shows the variation of the real and imaginary parts of the acoustic pressure along the upper inlet wall for a frequency of 1.0. The radial variation of the acoustic pressure at the inlet entrance plane, inlet throat, and inlet exit plane for $\omega = 1$ are shown in Figs. 6, 7, and 8, respectively. Similar plots for an axisymmetric plane wave excitation with $\omega = 2.0$ are shown in Figs. 9-12.

Within the assumption of this analysis, three effects on sound propagation in the turbofan inlet will be observed; 1) reflection of sound from the inlet walls due to variation in the cross-sectional area, and possibly reflection from the entrance plane due to specification of a "simple" impedance condition; 2) convection of sound by the mean flow which affects the local effective wavelength; and 3) refraction of sound by the mean flow, which refers to the tendency of transverse gradients in the mean flow to induce wave motion normal to the duct axis.

When the mean flow is described by a one-dimensional approximation, only reflection and convection will be important. Furthermore, in this case, the inlet impedance, $Z = 1$, is a good approximation for the no-reflection condition at the entrance plane and thus only reflection from the walls should be present. Figures 6-8 and 10-12 show very little distortion in the plane wave shape (for one-dimensional mean flow) indicating that there is very little reflection from the inlet walls.

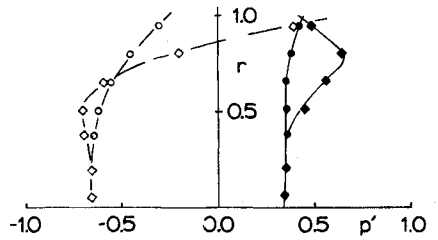

Fig. 10 Radial variation of acoustic pressure at the entrance plane for $\omega = 2.0$ (symbols defined in Fig. 5).

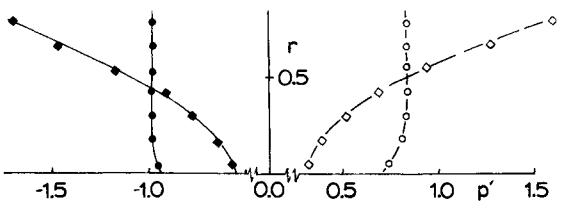

Fig. 11 Radial variation of acoustic pressure at the throat plane for $\omega = 2.0$ (symbols defined in Fig. 5).

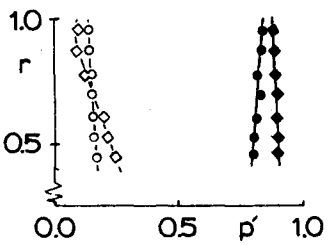

Fig. 12 Radial variation of acoustic pressure at the inlet exit (fan) plane for $\omega = 2.0$ (symbols defined in Fig. 5).

Figures 5 and 9 show the convective effects, as manifested by the decrease in the effective wavelength near the throat where the higher mean-flow Mach numbers exist.

When the mean flow is described by a two-dimensional approximation, all three effects are present. Furthermore, at the inlet entrance plane, radial mean flow velocities are quite large and there are radial gradients in the axial component of the mean flow. Under these conditions, the assumed impedance of $Z = 1$ will result in wave reflection at the inlet entrance plane. For the two-dimensional mean flow description, Figs. 6-8 and 10-12 show severe distortion in the initially plane wave shape due to refraction, convection, and reflection from the entrance plane. Figures 5 and 9 show a change in the effective wavelength. Due to the complex interaction between the reflection, convection, and refraction, it is not possible to isolate the individual effects. It is known,[1,23] however, that refraction increases with an increase in frequency. This effect is observed by comparing Figs. 6-8 (for $\omega = 1.0$) and Figs. 10-12 (for $\omega = 2.0$), where the distortion of the plane wave front increases with an increase in frequency.

In summary, comparison between known analytical solutions and results obtained using the developed FEM show that the latter is indeed working properly. These computations have shown that the accuracy of the FEM has deteriorated, as the frequency of the wave increased while the number of elements remained fixed. Inlet acoustic studies performed with two- and one-dimensional mean flow descriptions have provided different acoustic predictions for these two cases. It has also been shown that gradients in the mean flow resulted in considerable distortion of the original plane wave excitation.

Acknowledgment

This research was sponsored by NASA Lewis Research Center under NASA Grant NSG 3036.

References

[1] Nayfeh, A. H., Kaiser, J. E., and Telionis, D. P. "Acoustics of Aircraft Engine-Duct Systems," AIAA Paper 73-1153, 1973; also, *AIAA Journal*, Vol. 13, Feb. 1975, pp. 130-153.

[2] Quinn, D. W., "A Finite Difference Method for Computing Sound Propagation in Nonuniform Ducts," AIAA Paper 75-130, 1975; also, *AIAA Journal*, Vol. 13, Oct. 1975, pp. 1392-1393.

[3] Bell, W. A., Meyer, W. L., and Zinn, B. T., "Predicting the Acoustic Properties of Arbitrarily Shaped Bodies by Use of an Integral Approach," AIAA Paper 76-494, 1976; also, *AIAA Journal*, Vol. 15, June 1977, pp. 813-820.

[4] Hogge, H. D. and Ritzi, E. W., "Theoretical Studies of Sound Emission from Aircraft Ducts," Douglas paper 6191, presented to AIAA Aero-Acoustics Conference, Seattle, Wash., 1973.

[5] Tam, C. K. W., "Transmission of Spinning Acoustic Modes in a Slightly Non-Uniform Duct," *Journal of Sound and Vibration*, Vol. 18, March 1971, pp. 339-351.

[6] Nayfeh, A. H., Kaiser, J. E., and Telionis, D. P., "Transmission of Sound through Annular Ducts of Varying Cross Section," *AIAA Journal*, Vol. 13, Jan. 1975, pp. 60-65.

[7] Sigman, R. K., Majjigi, R. K., and Zin, B. T., "Use of Finite Element Techniques in the Determination of the Acoustic Properties of Turbofan Inlets," AIAA Paper 77-18, Los Angeles, Calif., Jan., 1977.

[8] Eversman, W., Astley, R. J., and Thanh, V. P., "Transmission in Nonuniform Ducts – A Comparative Evaluation of Finite Element and Weighted Residuals Computational Schemes," AIAA Paper 77-1299, Atlanta, Ga., Oct. 1977.

[9] Watson, W. R., "Finite Element Analysis of Sound Propagation in a Rectangular Duct of Finite Length with Peripherally Variable Liners," AIAA Paper 77-1300, Atlanta, Ga., Oct. 1977.

[10] Abrahamson, A., "A Finite Element Model of Sound Propagation in a Non-Uniform Circular Duct Containing Compressible Flow," AIAA Paper 77-1301, Atlanta, Ga., Oct. 1977.

[11] Huebner, K. H., *The Finite Element Method for Engineers*, John Wiley and Sons, Inc., New York, 1975.

[12] Bisplinghoff, R. L., Ashley, H., and Halfman, R. L., *Aeroelasticity*, Addison-Wesley Publishing Co., Inc. Reading, Mass, 1955.

[13] Tyler, J. M. and Sofrin, T. G., "Axial Flow Compressor Noise Studies," *SAE Transactions*, Vol. 70, 1962, pp. 303-332.

[14] Rice, E. J., "Attenuation of Sound in Soft-Walled Circular Ducts," *Aerodynamic Noise*, edited by H. S. Ribner, Univ. of Toronto Press, 1969, pp. 229-249.

[15] Wu, J. C., Sigman, R. K., Hubbartt, J. E., and McMahon, H. M., "Potential Flow Studies of Lift-Fan Inflow Interference Phenomena," Aerospace Research Labs, ARL 73-0132, Oct. 1973.

[16] Lieblin, S. and Stockman, N. O., "Compressibility Corrections for Internal Flow Solutions," *Journal of Aircraft*, Vol. 9, April 1972, pp. 312-313.

[17] Hess, J. L. and Smith, A. M. O., "Calculation of Potential Flow About Arbitrary Bodies," *Progress in Aeronautical Sciences*, Vol. 8, Pergamon Press, 1967, pp. 1-138.

[18] Pipes, L. A. and Harvill, L. R., *Applied Mathematics for Engineers and Physicists*, 3rd Ed., McGraw-Hill, New York, 1958, p. 44.

[19] *Math Science Library*, published by Control Data Corporation, Vol. VI, 1973.

[20] Miller, B. A., Dastoli, B. J., and Wesoky, H. L., "Effect of Entry-Lip Design on Aerodynamics and Acoustics of High-Throat-Mach-Number Inlets for the Quiet, Clean, Short-Haul Experimental Engine" NASA TM X-3222, May 1975.

[21] Baumeister, K. J., "Generalized Wave Envelope Analysis of Sound Propagation in Ducts with Stepped Noise Source Profiles and Variable Axial Impedance," NASA TM X-71674, March 1975.

[22] Liepmann, H. W. and Roshko, A., *Elements of Gasdynamics*, John Wiley and Sons, Inc., New York, 1957.

[23] Tack, D. H. and Lambert, R. F., "Influence of Shear Flow on Sound Attenuation in a Lined Duct," *The Journal of Acoustical Society of America*, Vol. 38, Jan. 1951, pp. 39-45.